Asp-Gly Based Peptides Confined at the Surface of Cationic Gemini Surfactant Aggregates

Aurélie Brizard, Christel Dolain, Ivan Huc, and Reiko Oda*

Institut Européen de Chimie et Biologie, 2 rue Robert Escarpit, 33607 Pessac Cedex, France

Received December 30, 2005. In Final Form: February 12, 2006

Cationic gemini surfactants complexed with anionic oligoglycine-aspartate (called gemini peptides hereafter) were synthesized, and their aggregation behaviors were studied. The effects of the hydrophobic chain length (C10−C22) and the length of the oligoglycine (0−4) were investigated, and it was clearly shown by critical micellar concentration, Krafft temperature, and isothermal surface pressure measurements that the hydrophobic effect and interpeptidic interaction influence the aggregation behavior in a cooperative manner. Below their Krafft temperatures, some of them formed both hydro- and organogels with three-dimensional networks and the Fourier transform infrared measurements show the presence of interpeptidic hydrogen bonds.

Introduction

The confinement of molecules capable of molecular recognition at the surface of nanometric supramolecular objects is an interesting way of reinforcing intermolecular and intersupramolecular interactions. Such an approach allows induction of recognition mechanisms between functionalized supramolecular objects but also the nanoscale control of the morphology of molecular assemblies (bottom-up architecture). In this context, designing of structurally well-defined assemblies[1] inspired by biological systems is particularly attractive.

Confinement of peptides at a surface can induce structure formations and the use of peptidic lipids has been proposed in such a context, aiming at induced structure and functionality of such assemblies that may not be present or may organize differently in free solution.[2] A number of examples are found in the literature, reporting various induced interactions and conformations between short peptides confined at the surface of amphiphilic molecules.[3,4]

Almost all of these systems use peptidic lipids where the peptides are covalently connected to amphiphilic molecules. Herein we report a new family of peptido amphiphiles formed by the complexation of cationic surfactants and anionic oligopeptides, acetyl-$(Gly)_p$-aspartate. Their behavior in bulk solution as well as at the air−water interface was investigated. As cationic surfactants, dimeric (gemini) surfactants comprised of two conventional single-tail surfactants connected covalently at their headgroups were used. These surfactants show quite unusual phase behaviors and have recently motivated numerous physicochemical and biophysical studies.[5] The most studied class of cationic gemini amphiphiles are bis-quaternary ammonium surfactants having the formula C_sH_{2s}-α,ω-$((CH_3)_2N^+C_mH_{2m+1}$-$Br^-)((CH_3)_2N^+C_mH_{2m+1}Br^-)$ denoted with *m*-*s*-*m* notation.[6] For this group of surfactants, the effects of various structural variations on their assembling morphologies and physicochemical properties are reported.[7]

We have recently shown that the chiral counterion tartrate can induce supramolecular chirality to the membranes formed with nonchiral gemini amphiphiles. Such molecules self-assemble in solution to form chiral fibers with their sizes and helical pitch ranging from tens of nanometers to microns. These fibers form three-dimensional networks gelling organic and aqueous solvents.[8] Infrared and NMR spectroscopies have shown that the intimate interaction between the amphiphilic molecules and the tartrate counterions influence the molecular conformation of gemini molecules and there is a cooperative effect between the organization of amphiphilic molecules and that of counterions.[9]

For the present study, we have chosen the same gemini surfactants with an ethylene spacer (*n*-2-*n*)[10] with various chain lengths that were complexed with oligopeptides by ion exchange as shown in Scheme 1. The conditions were chosen such that one peptide acetyl-$(Gly)_p$-Asp (denoted as $AcGly_pAsp$) forms a complex with one gemini molecule.

The reasons for choosing such molecules were as follows. First, it is easier to obtain peptide amphiphiles with different peptide or hydrophobic chain lengths by cation−anion complexation as opposed to synthesizing new molecules each time.

(1) Lowe, C. R. *Curr. Opin. Struct. Biol.* **2000**, *10*, 428.
(2) (a) Yu, Y.-C.; Tirrell, M.; Fields, G. B. *J. Am. Chem. Soc.* **1998**, *120*, 9979. (b) Forns, P.; Lauer-Fields, J. L.; Gao, S.; Fields, G. B. *Biopolymers* **2000**, *54*, 531.
(3) (a) Santoso, S. S.; Vauthey, S.; Zhang, S. *Curr. Opin. Colloid Interface Sci.* **2002**, 262. (b) Yamada, N.; Imai, T.; Koyama, E. *Langmuir* **2001**, *17*, 961. (c) Yamada, N.; Matsubara, K.; Narumi, K.; Sato, Y.; Koyama, E.; Ariga, K. *Colloids Surf., A: Physicochem. Eng. Aspects* **2000**, *169*, 271. (d) Ihara, H.; Fukumoto, T.; Hirayama, C.; Yamada, K. *Polym. Commun.* **1986**, *27*, 282. (e) Yamada, N.; Koyama, E.; Imai, T.; Matsubara, K.; Ishida, S. *J. Chem. Soc., Chem. Commun.* **1996**, 2297. (f) Yamada, N.; Ariga, K.; Naito, M.; Matsubara, K.; Koyama, E. *J. Am. Chem. Soc.* **1998**, *120*, 12192. (g) Shimizu, T.; Kogiso, M.; Masuda, M. *J. Am. Chem. Soc.* **1997**, *119*, 6209. (h) Kunitake, T. *Angew Chem., Int. Ed. Engl.* **1992**, *31*, 709. (i) Neumann, R.; Ringsdorf, H.; Patton, E. V.; O'Brien, D. F. *Biochim. Biophys. Acta* **1987**, *898*, 338. (j) Hartgerink, J. D.; Beniash, E.; Strupp, S. I. *Proc. Natl. Acad. Sci. U.S.A.* **2002**, *99*, 5133. (k) Shimizu, T.; Kogiso, M.; Masuda, M. *Nature* **1996**, *383*, 483.
(4) Löwik, D. W. P. M.; van Hest, J. C. M. *Chem. Soc. Rev.* **2004**, *33*, 234. and references therein.
(5) For reviews, see: (a) Rosen, M. J.; Tracy, D. J. *J. Surfactants Deterg.* **1998**, *1*, 547. (b) Menger, F. M.; Keiper, J. *Angew. Chem., Int. Ed.* **2000**, *39*, 1906. (c) *Gemini surfactants*; Zana, R., Xia, J., Eds.; Marcel Dekker: New York, 2004.
(6) Zana, R. *Adv. Colloid Interface Sci.* **2002**, *97*, 205.
(7) (a) Frindi, M.; Michels, B.; Levy, H.; Zana, R. *Langmuir* **1994**, *10*, 1140. (b) Alami, E.; Levy, H.; Zana, R.; Skoulios, A. *Langmuir* **1993**, *9*, 940. (c) De, S.; Aswal, V. K.; Goyal, P. S.; Bhattacharya, S. *J. Phys. Chem. B* **1998**, *102*, 6152. (d) Kim, T.-S.; Kida, T.; Nakatsuji, Y.; Hirao, T.; Ikeda, I. *J. Am. Oil Chem. Soc.* **1996**, *73*, 907. (e) Rosen, M. J.; Song, L. D. *J. Colloid Interface Sci.* **1996**, *179*, 261. (f) Bhattacharya, S.; De, S. *Langmuir* **1999**, *15*, 3400. (g) In, M.; Bec. V.; Aguerre-Chariol, O.; Zana, R. *Langmuir* **2000**, *16*, 141.
(8) (a) Oda, R.; Huc, I.; Candau, S. J. *Angew. Chem., Int. Ed.* **1998,** *37*, 2689. (b) Oda, R.; Huc, I.; Schmutz, M.; Candau, S. J.; MacKintosh, F. C. *Nature* **1999**, *399*, 566.
(9) Berthier, D.; Buffeteau, T.; Léger, J.-M.; Oda, R.; Huc I. *J. Am. Chem. Soc.* **2002**, *124*, 13486.
(10) (a) Oda, R.; Huc, I.; Homo, J.-C.; Heinrich, B.; Schmutz, M.; Candau, S. J. *Langmuir* **1999**, *15*, 2384. (b) Oda, R.; Huc, I.; Candau, S. J. *Chem. Commun.* **1997**, 2105.

10.1021/la053516a CCC: $33.50
Published on Web 03/09/2006

Scheme 1. (a) Gemini Peptide *n*-2-*n* AcGly$_p$Asp (Sometimes Denoted as *n*Gly$_p$ in the Text) and (b) AcGly$_{p+1}$Na

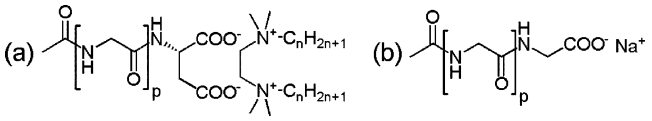

This is quite important when one wants to compare the properties of various peptide lengths or sequences. For the cation side, gemini molecules having *n*-2-*n* structure tend to form aggregates with low interfacial curvature (cylindrical micelles, bilayers, etc.)[11] at very low concentrations (~mM) compared to their monomeric counterparts,[10b] which is interesting from the point of view of structural studies. For the structure of oligopeptides, glycine was chosen since oligoglycines are the most labile peptides and the induction of structure would be the most efficient. The N-terminals of glycines were acetylated so that globally the peptides are anionic. C-terminals were complexed with aspartic acid, because of their dianionic character: with the two carbons between two carboxylic acids there is good matching with the distance between ammonium cations having an ethylene spacer. Such a structural matching has previously been shown to be important with the gemini tartrate complex.[8a] The effects of structural variation of such gemini oligoglycines on their molecular and supramolecular organization are presented: the ensemble of surface pressure isotherm, critical micellar concentration (cmc), and Krafft temperature (T_k) measurements demonstrates that the structure of counterions strongly influenced the intermolecular interaction of the aggregates. These molecules form an ambidextrous gelling agent, and Fourier transform infrared spectroscopy (FT-IR) clearly shows the presence of hydrogen bonding between the peptidic counterions.

Experimental Section

Oligopeptides. *N*-Acetyl-L-aspartic acid and Glycyl-L-aspartic acid were purchased from Fluka and used without further purification. *N*-Acetyl-glycylglycyl-L-aspartic acid was synthesized by coupling in solution *N*-acetyl-glycylglycine (obtained from glycylglycine, ACROS Organics) and l-aspartate dibenzyl ester obtained from L-aspartic acid dibenzyl ester toluene-4-sulfonate (Fluka). *N*-Acetyl-tetraglycyl-L-aspartic acid was directly prepared by solid-phase synthesis (COMIPSO, Bordeaux).

Acylation of Glycyl-L-aspartic Acid and Glycylglycine. *N*-Acetyl-oligopeptides were prepared by adding the peptide (200 mg) to a solution of acetic acid (10 mL) and acetic anhydride (5 mL). The mixture was vigorously stirred at room temperature for 24 h. After evaporation of the solvent under vacuum, 10 mL of water was added to hydrolyze the terminal acidic function. Consecutive lyophilization and dissolution in water were repeated to ensure complete evaporation of acetic acid (controlled by ^{1}H NMR)

AcGlyAsp. ^{1}H NMR (400 MHz, DMSO, 25 °C, δ ppm): 8.18 (1H, d, ^3J = 8.08 Hz); 8.11 (1H, t, ^3J = 5.81); 4.53 (1H, dt, ^3J = 8.02 Hz, ^3J = 6.21 Hz); 3.69 (2H, d, ^3J = 5.81 Hz); 2.68 (1H, dd, ^2J = 16.67 Hz; ^3J = 5.81 Hz); 2.57 (1H, dd, ^2J = 16.67 Hz; ^3J = 6.28 Hz); 1.84 (3H, s). ^{13}C NMR (100 MHz, DMSO, 25 °C, δ ppm): 172.28; 171.70; 169.51; 168.91; 48.46; 41.68; 36.01; 22.46.

AcGlyGly. ^{1}H NMR (400 MHz, DMSO, 25 °C, δ ppm): 8.15 (2H, m); 3.75 (2H, d, ^3J = 5.81 Hz); 3.70 (1H, d, ^3J = 5.81 Hz); 1.86 (3H, s). ^{13}C NMR (100 MHz, DMSO, 25 °C, δ ppm): 171.17; 169.60; 169.46; 41.81; 40.56; 22.53.

Coupling of *N*-Acetyl-glycylglycine with L-Aspartate Dibenzyl Ester. L-Aspartate dibenzyl ester (1.1 equiv) was extracted from L-aspartic acid dibenzyl ester toluene-4-sulfonate (1.1 equiv, 500 mg) by an ether/$NaHCO_3$ saturated solution. The organic phase was separated and dried on $MgSO_4$; the ether was evaporated just before the use of the resulting product for the coupling. Simultaneously, *N*-acetyl-glycylglycine (162.8 mg, 1 equiv) and 1-hydroxybenzotriazole (HOBT) (143.2 mg, 1 equiv) were dissolved in 10 mL of dimethylformamide (DMF). *N*,*N*-Diisopropylethylamine (0.95 equiv) and 1-*H*-benzotriazolium, 1-[bis(dimethylamino)methylene]-hexafluorophosphate (1-), 3-oxide (HBTU) (0.98 equiv) were added to the previous mixture, which was stirred for 20 min at room temperature (RT). Then, L-aspartate dibenzyl ester (1.1 equiv) dissolved in 2 mL of DMF was added, and the resulting mixture was vigorously stirred for 24 h, at RT. The final product was extracted with ethyl acetate and $NaHCO_3$ saturated water. The resulting organic phase was then treated by dilute acetic acid solution, washed several times with water, dried on $MgSO_4$, and filtered, and the solvent was evaporated under vacuum.

AcGly$_2$AspBn$_2$. ^{1}H NMR (400 MHz, DMSO, 25 °C, δ ppm): 8.5 (1H, d, ^3J = 7.68 Hz); 8.19 (2H, m, ^3J = 5.81); 7.35 (10H, m); 5.08 (4H, d); 4.75 (1H, m); 3.73 (2H, d, ^3J = 4,75 Hz); 3.69 (2H, d, ^3J = 5,67 Hz), 2.92 (1H, dd, ^2J = 16.64 Hz; ^3J = 5.91 Hz); 2.57 (1H, dd, ^2J = 16.64 Hz; ^3J = 6.95 Hz); 1.85 (3H, s).

Catalytic Hydrogenation of *N*-Acetyl Glycylglycyl-L-aspartate Dibenzyl Ester. *N*-Acetyl glycylglycyl-L-aspartate dibenzyl ester (300 mg) was dissolved in 5 mL of trifluoroacetic acid (TFA), in the presence of 10% Pd/C (mass). The mixture was placed under hydrogen and vigorously stirred (4 h, RT). TFA was then evaporated under vacuum. Consecutive lyophilization and dissolution in water were repeated to ensure evaporation of trifluoroacetic acid (controlled by infrared).

AcGly$_2$Asp. ^{1}H NMR (400 MHz, DMSO, 25 °C, δ ppm): 8.18 (1H, d, ^3J = 8.08 Hz); 8.11 (1H, t, ^3J = 5.81); 4.53(1H, dt, ^3J = 8.02 Hz, ^3J = 6.21 Hz); 3.69 (2H, d, ^3J = 5.81 Hz); 2.68 (1H, dd, ^2J = 16.67 Hz; ^3J = 5.81 Hz); 2.57 (1H, dd, ^2J = 16.67 Hz; ^3J = 6.28 Hz); 1.84 (3H, s). ^{13}C NMR (100 MHz, DMSO, 25 °C, δ ppm): 172.17; 171.56; 169.72; 169.23; 48.43; 42.05; 41.52; 35.93; 22.40. Mass spectrometry (M + 1)/z = 290.1.

***n*-2-*n* AcGly$_p$Asp Synthesis (n = 12−22, p = 0−4): Ion Exchanges.** The *n*-2-*n* amphiphiles with bromide counterions were synthesized as previously reported.[10b] Various procedures for bromide to oligopeptide ion exchange were tested, to achieve the best results. We have observed that the presence of residual bromide—even less than 2%—may have a dramatic effect on the properties of the prepared gemini, implying that the stoichiometry between cationic gemini and anionic peptides must be carefully respected (unpublished results).

Method a. Ion-Exchange Column. The solution of gemini bromide in water/methanol mixture passes through a anion-exchange resin with hydroxide anions (Dowex 1_8, 50 ± 100 mesh, 20 equiv). The resulting gemini hydroxide was mixed with 1 equiv of oligopeptide, and the solution was lyophilized. The final product was dissolved in a mixture of chloroform/methanol (9/1, v/v), precipitated with ether, filtered, and dried.

Method b. Via Silver Peptide (Water). A suspension of the silver salt of the peptide in deionized water was prepared before each use upon mixing the peptide acid and Ag_2CO_3 (1 equiv), followed by vigorous stirring under slight vacuum for 1 h. A hot solution of the *n*-2-*n* surfactant (1 equiv, typically 50−100 mg scale) was added, and the mixture was stirred for 30 min at 40−50 °C and lyophilized. The resulting powder was dissolved in MeOH and filtered on Celite to give a colorless solution. After evaporation, the product was dissolved in a mixture of chloroform/methanol (9/1, v/v), precipitated with ether, filtered, and dried.

Mehtod c. Via Silver Peptide (MeOH). The method was the same as the previous method except that peptides were solubilized in methanol. As a consequence, after the addition of the *n*-2-*n* surfactant (also in methanol) to the mixture, the AgBr dark powder could be directly filtered on Celite.

^{1}H NMR revealed a lack of 2−5% of peptidic anions with method a. This is probably due to the high viscosity of gemini *n*-2-*n* solution in water when $n \geq 14$, preventing efficient exchange of bromide by hydroxide. Moreover, once exchanged, gemini molecules turned out to be unstable in basic solution (pH >10).[12] When methods b

(11) Israelachvili, J. *Intermolecular & Surface Forces*, 2nd ed.; Academic Press: London, 1992.

(12) Berthier, D. Ph.D. Thesis, University of Bordeaux I, 2002.

and c were compared, the intermediate product of silver salt of peptide seems to have a higher solubility in methanol; thus method c results in a gemini peptide with better stoichiometry.[13]

18-2-18 AcGly$_0$Asp. ^{1}H NMR (400 MHz, CD_3OD, 25 °C, δ ppm): 4.47 (1H, t, ^3J = 4,87 Hz); 3.93 (4H, s); 3.42 (4H, m); 3.22 (12H, s); 2.70 (1H, dd, ^2J = 16.06 Hz; ^3J = 4.87 Hz); 2.64 (1H, dd, ^2J = 16.06 Hz; ^3J = 4.87 Hz); 1.99 (3H, s); 1.83 (4H, m); 1.43 (4H, m); 1.30 (56H, m); 0.91 (6H, t, ^3J = 6.56 Hz). ^{13}C NMR (100 MHz, CD_3OD, 25 °C, δ ppm): 178.67; 178.33; 171.74; 66.41; 56.76; 53.30; 51.56; 40.84; 32.77; 30.52; 30.48; 30.42; 30.34; 30.19; 30.10; 27.08; 23.47; 23.15; 14.43.

18-2-18 AcGly$_1$Asp. ^{1}H NMR (400 MHz, CD_3OD, 25 °C, δ ppm): 4.47 (1H, t, ^3J = 4,87 Hz); 3.92 (4H, s); 3.90 (2H, m); 3.42 (4H, m); 3.22 (12H, s); 2.71 (1H, dd, ^2J = 15.66 Hz; ^3J = 4.87 Hz); 2.64 (1H, dd, ^2J = 15.66 Hz; ^3J = 4.87 Hz); 2.03 (3H, s); 1.83 (4H, m); 1.44 (4H, m); 1.30 (56H, m); 0.92 (6H, t, ^3J = 6.56 Hz). ^{13}C NMR (100 MHz, CD_3OD, 25 °C, δ ppm): 179.05; 178.72; 173.39; 170.64; 66.67; 56.99; 53.96; 51.88; 43.80; 41.19; 33.09; 30.82; 30.78; 30.73; 30.63; 30.50; 30.38; 27.36; 23.71; 22.71; 14.48.

18-2-18 AcGly$_2$Asp. ^{1}H NMR (400 MHz, CD_3OD, 25 °C, δ ppm): 4.45 (1H, t, ^3J = 5,30 Hz); 3.92 (4H, s); 3.90 (4H, m); 3.43 (4H, m); 3.22 (12H, s); 2.70 (1H, dd, ^2J = 16.42 Hz; ^3J = 5.30 Hz); 2.64 (1H, dd, ^2J = 16.42 Hz; ^3J = 5.30 Hz); 2.04 (3H, s); 1.84 (4H, m); 1,44 (4H, m); 1,30 (56H, m); 0,92 (6H, t, ^3J = 6,56 Hz). ^{13}C NMR (100 MHz, CD_3OD, 25 °C, δ ppm): 178.99; 178.75; 173.84; 172.11; 170.54; 66.68; 56.97; 54.02; 51.89; 43.71; 43.52; 41.01; 33.088; 30.78; 30.72; 30.63; 30.50; 30.38; 27.37; 23.75; 23.71; 22.66; 14.46.

18-2-18 AcGly$_4$Asp. ^{1}H NMR (400 MHz, CD_3OD, 25 °C, δ ppm): 4.47 (1H, t, ^3J = 5,26 Hz); 3.97 (4H, s); 3.96 (8H, m); 3.44 (4H, m); 3.23 (12H, s); 2.74 (1H, dd, ^2J = 16.92 Hz; ^3J = 5.56 Hz); 2.67 (1H, dd, ^2J = 16.92 Hz; ^3J = 5.56 Hz); 2.05 (3H, s); 1.85 (4H, m); 1,44 (4H, m); 1,31 (56H, m); 0,92 (6H, t, ^3J = 6,36 Hz). ^{13}C NMR (100 MHz, CD_3OD, 25 °C, δ ppm): 178.96; 178.73; 174.15; 172.76; 172.40; 171.96; 170.55; 66.74; 56.98; 53.92; 51.90; 43.86; 43.65; 43.57; 33.09; 30.82; 30.78; 30.72; 30.63; 30.50; 30.37; 27.37; 23.75; 23.72; 22.63; 14.46.

Conductivity Measurements. The conductivity was measured with a Consort C830 (Belgium) conductimeter with an SK10T platinum electrode embedded in glass (cell constant 1.0 cm^{-1}). The measurements were performed in a temperature-controlled double-walled glass container with a circulation of water.

For the cmc measurements, a stock solution of surfactant at a concentration about 10 times the expected cmc was successively added to 4 mL of deionized water (Purelab Prima Elga, 18.2 MΩ• cm). Sufficient time was given between additions (>1 min) until the conductivity reached equilibrium after each addition.

The Krafft temperatures were also determined using the electrical conductivity method[14] combined with visual observation. Since the conductivity is strongly influenced by the presence of any metastable and kinetically controlled aggregates, care was taken so that all samples are treated in the same manner. The powder of surfactant was first solubilized in water to obtain the solution of about 1% w/w, and then it was freeze-dried to get a very fine powder. This powder was again dispersed in water to obtain 3 mM solutions, much above the cmc of all the investigated surfactants. For some of the solutions, either the kinetics of precipitation was extremely slow or gel formation instead of precipitation was observed. To make sure that all the samples formed well hydrated precipitate, the solutions were plunged into liquid nitrogen to get fast congelation, and then they were kept at 2 °C for several hours so that they melted without forming a gel. The solutions with precipitates were introduced into the conductivity cell, and the conductivity was measured as the temperature was increased between 2 and 80 °C with a temperature increase rate of 1 °C per 10 min. The Krafft temperature was taken at the temperature where the specific conductance (μS/cm) versus temperature plot showed a break after a sharp increase. This break usually coincided with the temperature of full clarification of the system.

Surface Pressure Measurements. The surface pressure measurements were performed on a computer-controlled Langmuir film balance (Nima Technology, Coventry, UK), and the surface pressure (π) was measured by the Wilhelmy method using a filter paper plate (10 × 23.5 mm). Care was taken so that, during the measurements, the bottom edge of the well-soaked plate was always just at water surface level, still attached to the meniscus.

For the surface pressure isotherms, a rectangular Teflon trough with computer-controlled barriers with a compression rate of 5 × 70 = 350 cm^2 was used. The trough was filled with ultrapure water with the temperature controlled at $T = 21 \pm 2$ °C. The compression rate was 5 cm^2/min and data points were taken about every 0.05 Å^2.

Amphiphiles were solubilized in a mixture of chloroform/methanol to make solutions on the order of 10^{-4} mol/L. The ratio of two solvents depended on the solubility of the molecules. A carefully measured quantity (on the order of 50 μL) of the solutions was spread at the air−water interface with Hamilton syringes. After waiting for 10 min to let the solvents evaporate, the compression curves were registered. The isotherm curves for all the molecules and the mixtures of molecules were repeated at least 3 times and were found to show good reproducibility: the standard deviations of the limiting molecular areas as well as the molecular areas at collapse were less than 5 Å^2 and the deviations of the surface pressures at the collapse points were less than 5 mN/m.

FT-IR Spectroscopy Measurements. The FT-IR spectra were recorded on a Bruker IFS 55 FT-IR spectrometer (Bruker, Karlsruhe, Germany) equipped with a detector (DKATGS with KBr window). To avoid the big absorption peak of H_2O, which hides the amide I peaks, solutions in D_2O were prepared. Generally, 100 scans were added at a resolution of 4 cm^{-1}. The transmission measurements were performed with two ZnSe windows.

Scanning Electron Microscopy. Hydrated samples (10 μL) were frozen in liquid propane (to avoid water crystallization) before being lyophilized. The obtained powders were coated with Au/Pd under vacuum and observed using a JEOL GSM 840A microscope operating at 15 kV.

Optical Microscopy with Differential Interferential Contrast (DIC). Samples were sealed between slide glass and cover glass and were observed with a NIKON Eclipse PhysioStation E600FN using a 100×/1.4 PlanFluor objective with an adequate condenser and a prism for DIC observations.

Small-Angle X-ray Scattering. A Rigaku Nanoviewer (Microsource generator, MicroMax 007, 800W rotating anode coupled with a Confocal Maxflux Mirror) was used. Gels were put between two Mylar windows with a spacer of 1 mm. The temperature of the samples was regulated at 18 °C unless indicated differently. Integrations of the spectra were performed with a program delivered with the apparatus.

Results

All the gemini formed a fluid solution at 10 mM upon heating above T_k. When the solutions were cooled to room temperature (controlled at 21 °C), some of them formed hydrogels[15] within a few hours. The Table 1 shows their gelling behavior at room temperature.

As can clearly be remarked, the gelling behavior is more pronounced for molecules with longer alkyl chains. All the gemini peptides with C20 and C22 formed gel both at room temperature and at 4 °C regardless of peptide numbers. On the other hand, for gemini peptides with chain lengths shorter than C14, all were soluble whatever the temperatures and peptide lengths. For C16, gel formation was observed only for $p = 0$ and 4, and only at

(13) To test the results of ion exchange, the following test was driven: a few milligrams of the gemini peptides was put in the presence of silver acetate ("cream colored"), in methanol. With methods a and b, the mixture became rapidly dark (less than 30 min), indicating the formation of AgBr and suggesting the presence of residual bromide. On the contrary, the gemini peptides synthesized via method c mixed with silver acetate remained clear, showing negligible amounts of residual bromide.

(14) (a) Saito, S.; Moroi, Y.. Matuura, R. *J. Colloid Interface Sci.* **1982**, *88*, 578. (b) Nishikido, N.; Kobayashi, H.; Tanaka, M. *J. Phys. Chem.* **1982**, *86*, 3170.

(15) Estroff, L. A.; Hamilton, A. D. *Chem. Rev.* **2004**, *104*, 1201.

Table 1. Behavior at 21 °C/2 °C of 10 mM Gemini Peptide Solutions with Various Hydrophobic Chain Lengths (C10−C22) and Peptide Lengths (p = 0, 1, 2, 4)[a]

	$n \leq 14$	$n = 16$	$n = 18$	$n = 20$	$n = 22$
$p = 0$ ($AcGly_0Asp$)	sol/sol	sol/gel	gel/gel	gel/gel	gel/gel
$p = 1$ ($AcGly_1Asp$)	sol/sol	sol/sol	sol/gel	gel/gel	gel/gel
$p = 2$ ($AcGly_2Asp$)	sol/sol	sol/sol	sol/gel	gel/gel	gel/gel
$p = 4$ ($AcGly_4Asp$)	sol/sol	sol/gel	gel/gel	gel/gel	gel/gel

[a] Sol = solution.

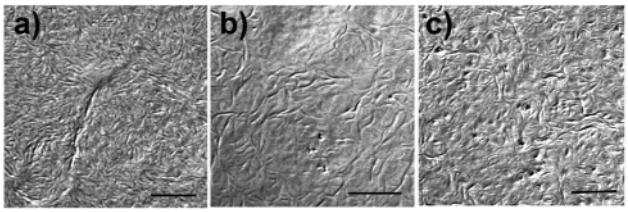

Figure 1. DIC microscope images of (a) 20-2-20 $AcGly_0Asp$, (b) 20-2-20 $AcGly_1Asp$, (c) 22-2-22 $AcGly_1Asp$; bar = 10 μm. These three images are the representative images of gels, showing fibrous structures. No particular sample-dependent differences in morphologies were observed.

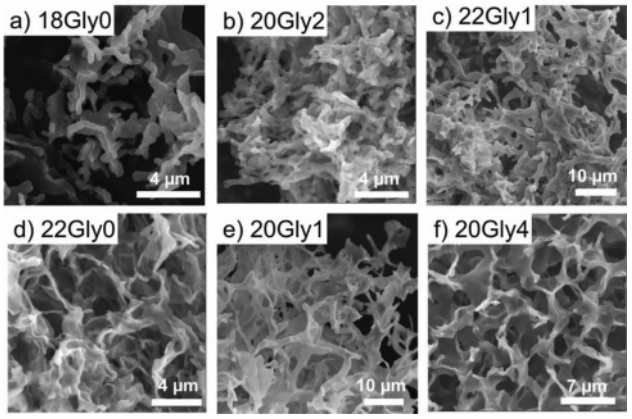

Figure 2. Lyophilized gels observed with SEM. Submicrometer-scale objects forming a three-dimensional network with no particular inner structures are observed. Some are formed with fibrous structures (a−c), and others are formed with more membrane-like structures (d−f).

4 °C. For C18, they all formed gels at 4 °C. On the other hand, at room temperature, the gel melted for $p = 1$ and 2.

The optical microscopic images of some of the gels at 50 mM show an entangled network of fibrillar structures with a diameter on the order of a few hundred nanometers (Figure 1).

Such an observation was then compared with the electron microscopic images. Despite numerous trials, transmission electron microscopy did not give satisfactory images. On the other hand, observation by scanning electron microscopy of gels frozen directly in liquid propane followed by lyophilization demonstrated three-dimensional networks of fibers of membrane-like structures (Figure 2). The diameters or the widths of these structures were on the order of 200−400 nm in agreement with optical microscopic observations, and they did not show apparent internal structure. The effect of the different chain lengths and peptide lengths on the fiber structure could not clearly be nailed down.

Krafft Temperature (T_k). The Krafft temperatures measured by conductimetry for four different chain lengths, C16, C18, C20, and C22, and for four different peptide lengths, $AcGly_pAsp$ (p = 0, 1, 2, 4), are shown in Figure 3.

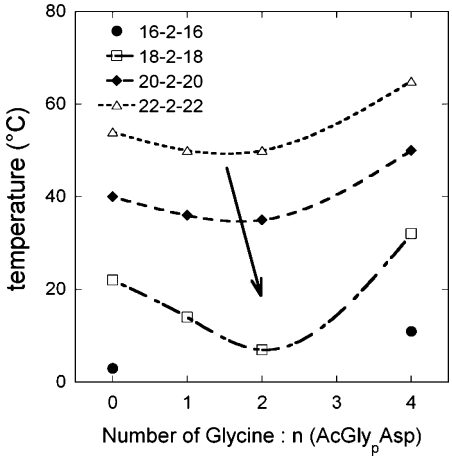

Figure 3. Krafft temperature of n-2-n $AcGly_pAsp$, as a function of glycine number p. 16-2-16 $AcGly_{1\text{ and }2}Asp$ are both soluble at 1 °C. Lines are guides for the eye.

For a fixed peptide length, the Krafft temperature showed a monotonic decrease with increase in the hydrophobic chain length. The variation is on the order of 10−20 degrees per two carbons, which is in good agreement with previously reported results with other gemini surfactants.[5c] On the other hand, the variation of T_k as a function of oligoglycine length at a fixed hydrophobic chain length showed a minimum around $p = 1-2$. Furthermore, it seems that the minimum shifts toward a higher p number as the chain length decreases.

cmc. Conductivity measurements were used to determine the cmc's of gemini oligoglycines. Because of the high hydrophobicity due to their dimeric nature, the determination of cmc's (on the order of 10^{-6} M) turned out to be difficult for C16−C20 gemini surfactants. Therefore, we used the gemini peptides with 10, 12, and 14 carbons with 0−4 glycines. In Figure 4, conductivity curves for 12-2-12 and 14-2-14 $AcGly_pAsp$, as summarized in Table 2, and the variation of cmc as a function of hydrophobic chain length for $AcGly_0Asp$ are shown. The cmc decreases about an order of magnitude as the carbon number increases by two per chain. On the contrary, the effect of the peptidic length at fixed hydrophobic chain lengths of C12 and C14 is very difficult to clearly nail down: because the differences are very small and the breaks in the curves are not very sharp, it is difficult to clearly determine the absolute values. If there is any cmc variation, however, it seems to show a tendency to decrease with the increase in peptide length.

Surface Pressure Isotherms. The interaction between gemini $AcGly_pAsp$ was studied at the air−water interface. In Figure 5a,b $\pi-A$ curves are shown for given hydrocarbon lengths C18 and 20 with various peptide lengths.[16] For both gemini $AcGly_p$-Asp molecules, the shapes of the curves were similar for all the peptide lengths, showing monotonic increases in the surface pressure until the collapse points. No intermediate transitions were observed. For 20-2-20 $AcGly_pAsp$ and $p = 1$ and 2, the collapse points were not easily defined because of the presence of a shoulder at about 90 Å^2. The characteristic values for each system are summarized in Figure 5c,d. It is interesting to note that the molecular areas do not vary linearly with the peptide length, but rather they have a maximum at $p = 1$ or 2 and the position of the maximum is observed at a higher peptide number for C18 than for C20.

(16) Since the molecules with C16 were too soluble and did not have a clear collapse and C22 had a phase transition that made it difficult to compare the different peptide lengths (Figure 10), we focused specifically on the systems with C18 and C20.

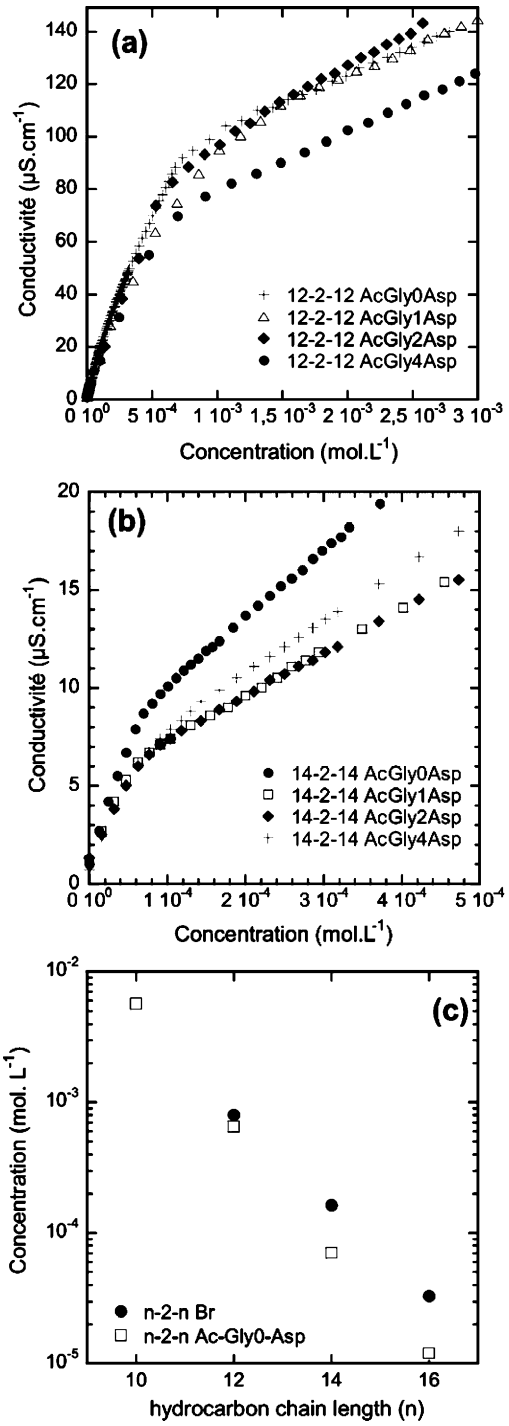

Figure 4. cmc determination by conductivity measurements for (a) C12 and (b) C14 for $p = 0-4$. The peptide length does not seem to have a big influence on the cmc values. It decreases about an order of magnitude as the chain length increases by two $(CH_2)_2$ as shown in (c) for $p = 0$. These values were also compared to gemini having bromide counterions. cmc values are slightly lower for gemini $AcGly_0Asp$.

The differences of molecular area observed between various glycine lengths at a fixed gemini chain length as described above are quite small (between 10 and 25 Å^2). To check that it is not an artifact, we performed surface pressure isotherm measurements of gemini (22-2-22) monolayers with a large excess of sodium salt of oligopeptides in the subphase. A monolayer of gemini acetate[17] was deposited on a subphase containing about 6000 equiv of $AcGly_pAsp$ sodium salt.

Table 2. cmc Values of *n*-2-*n* $AcGly_pAsp$ Measured by Conductimetry ($n = 10-16$ for $p = 0$; $n = 12$ and 14 for $p = 0-4$)

	$n = 12$	$n = 14$
$p = 0$	7.5×10^{-4} M	6.5×10^{-5} M
$p = 1$	7.3×10^{-4} M	7.0×10^{-5} M
$p = 2$	6.4×10^{-4} M	7.0×10^{-5} M
$p = 4$	6.0×10^{-4} M	7.0×10^{-5} M

In Figure 6a), four isotherm curves with different peptide lengths are compared, and in Figure 6b the areas per molecules at the surface pressure of 14 mN/m are compared. It is clearly shown that the molecular area is maximum for Gly_1 counterions, reaching about 130 Å^2 before decreasing to about 85 Å^2 for Gly_4. This behavior is in agreement with the observation with stoichiometric gemini peptides.

FT-IR Measurements. FT-IR measurements on 100 mM solutions and gels were performed to monitor inter- and intramolecular interactions as well as molecular organization. Here, we focused in particular on two domains in frequencies, one for the amide I bands of the amino acids around 1630−1680 cm^{-1}, and another domain for the symmetric and antisymmetric stretching bands ν_s and ν_{as} of CH_2 around 2850/2920 cm^{-1}. These two domains for various gemini $AcGly_pAsp$ are compared at different times after solubilization of molecules in D_2O. Figure 7 summarizes the positions of ν_{as} peaks of CH_2 and amide I of amino acids of gemini peptide (C16−C22, Gly_0-Gly_4) solution at 72 h after solubilization.

It is clear that, for those that do not form gels at room temperature, the frequencies associated with the stretching vibrations of the alkyl chains remain at high wavenumbers (>2920/2850 cm^{-1}) such as those for C16 and C18 Gly_1 and Gly_2. For the gels, the wavenumbers for these bands decreased (e.g., 2924 → 2918 cm^{-1}) as the gels were formed, indicating a high organization of the gemini molecules in gels. The time necessary for reaching the final values depended on the samples: for 16-2-16 $AcGly_4Asp$ and 18-2-18 $AcGly_{0\text{ and }4}Asp$ CH_2 vibrations, evolution from high wavenumbers to low wavenumbers took as long as 3 days. For other gels, they were already at these low values as soon as the gels were prepared. Simultaneously, for $p = 0$, 1, and 2, the wavenumber for amide I bands in solution was around 1642−1645 cm^{-1} with very little time evolution, whereas for those that formed gels, these bands decreased with time (typically 1645 cm^{-1} → 1637 cm^{-1}), indicating the presence of hydrogen bonds in the gel network. Interestingly, the time evolution for amide I band with gel formation was much slower than the stretching mode for the hydrocarbon chains

Gemini $AcGly_4Asp$ molecules show particular behaviors: i.e., on top of a band around 1643 cm^{-1}, another peak at 1670 cm^{-1} (Figure 8e) is present. This peak only appears in the hydrated state, and does not exist for the powder. This peak does seem to appear as a very slight shouldering even for gemini $AcGly_2$-Asp systems, but it is clearly enhanced for $AcGly_4Asp$ systems.

In Figure 9, we have compared these amide I peaks with those of gemini complexed with two acetylated oligoglycine counterions (called gemini $(AcGly_p)_2$). It is clear that gemini $(AcGly_{3\text{ or }4})_2$ did not show the same organization of the glycine; i.e., gemini $AcGly_{3\text{ or }4}$ did not show the peak at 1670 cm^{-1}.

(17) Acetate counterion is chosen for its low affinity with ammonium headgroups (manuscript in preparation); thus the exchange by the oligopeptides in solution will be more efficient.

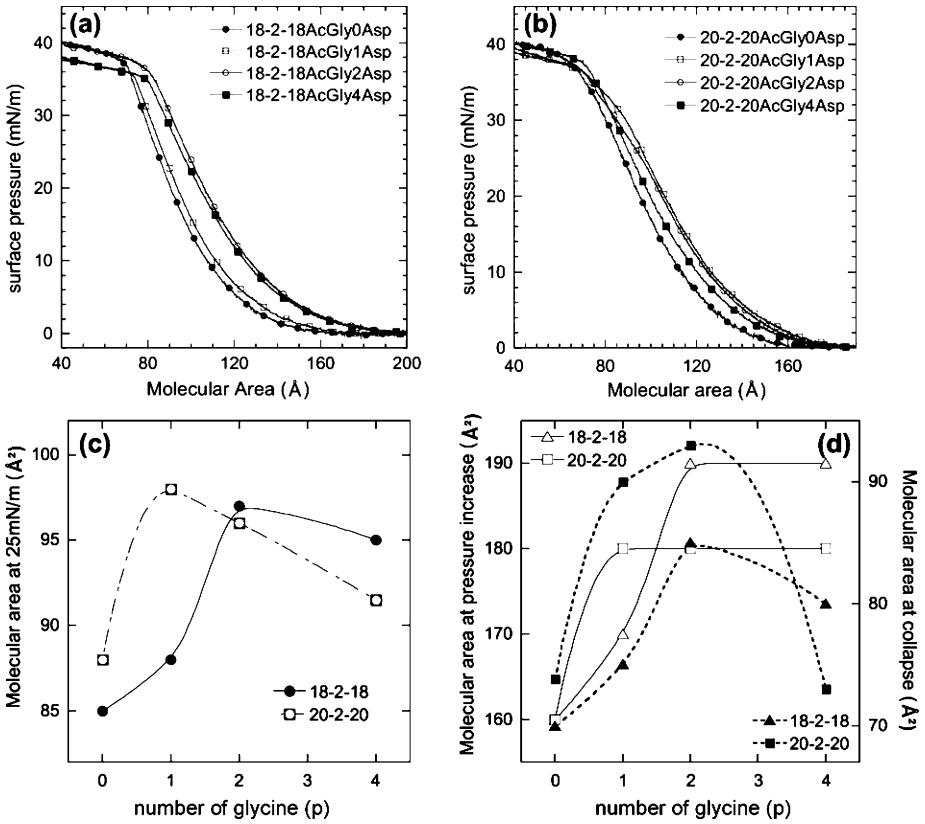

Figure 5. $\pi-A$ isotherm curves of *n*-2-*n* gemini surfactants where *n* is (a) 18 and (b) 20 for four different peptide lengths, $p = 0, 1, 2, 4$. Peptide length dependences on molecular area are shown (c) at surface pressure 25 mN/m, or (d) at the first detectable increase in surface pressure, and at collapse. Lines are guides for the eye.

In Figure 10, the effect of added $AcGly_5Na$ to the solution of 18-2-18 $AcGly_2Asp$ is shown. As previously discussed, 18-2-18 $AcGly_2Asp$ does not gel at room temperature, but upon addition of $AcGly_5Na$, it gels water. Both spectra of alkyl chains and spectra of amide I show better organization of gemini and peptides as seen by the decreasing wavenumbers of both peaks.

Small-Angle X-ray Scattering (SAXS). We compared hydrated gels (100 mM) and lyophilized (dried) gels. For all of them, a peak representing periodic stacking of bilayer structures was observed around 35−60 Å. In Figure 11, two series of graphs with peak positions for dehydrated and hydrated samples are shown.

As is commonly observed with this family of cationic gemini surfactants with ethylene spacer (unpublished results), the observed periodicity indicated that there were very little water between the membranes. Moreover, the effect of variation in hydrophobic chain length was clearly seen; i.e. as the chain gets longer, the periodicity increases by about 2−3 Å per $(CH_2)_2$.

From the IR measurements, we have observed that the hydrocarbon chains in gels are highly ordered and in the majority in trans conformation. If the hydrocarbon chain length can be roughly estimated as 1.2 Å × *n*, where *n* is the carbon number, for C18 the estimated thickness of bilayers would be at least 2 × 21.6 = 43.2 Å, for C20 = 48 Å, and for C22 = 52.8 Å. With the headgroups which will add at least 2 × 1.5 Å (2 × $N-CH_3$), these values, which furthermore do not take into account the counterions, were much higher than what was observed for dehydrated gels for low peptide numbers ($p = 0, 1, 2$). Probably the chains are tilted or interdigitated in the bilayer.

The effect of glycine length on the periodicity was much more complex. For the dehydrated gels, the periodicity increased with glycine number monotonically and the periodicity increase per glycine was about 3−4 Å, suggesting that glycines are organized perpendicular to the membrane. Upon hydration, for low peptide numbers the periodicity increased more than 15 Å, whereas for the high peptide numbers ($p = 4$) it decreased slightly. Therefore, they show minimum values at $p = 2$ for C22 and at $p = 4$ for C20. Such observations show that the molecular organization in particular for low peptide numbers is strongly influenced by the drying of the gels.

When compared to gemini $(AcGly_p)_2$, for the equivalent number of amino acids, for example $n = 20$ and 22 for *n*-2-*n* $(AcGly_3)_2$ vs *n*-2-*n* $AcGly_2Asp$, the gemini with two oligoglycine anions $(AcGly_3)_2$ had much higher periodicities. For example, the periodicity for 20-2-20 $(AcGly_3)_2$ = 68 Å and that for 20-2-20 $AcGly_2Asp$ = 47.5 Å.

The insertion of $AcGly_5Na$ influenced the solution of C18 $AcGly_{1\text{ and }2}Asp$ molecules quite dramatically. As shown by the IR and macroscopic observations, the fluid solution of C18 $AcGly_{1\text{ and }2}Asp$ gel upon addition of $AcGly_5Na$ accompanied the increase in organization of both hydrocarbon chains and peptides. SAXS measurements showed that the periodicity is increased by 6−7 Å, which strongly suggests that the oligoglycine salt is incorporated in the network of gemini glycine gels.

Discussion

The various techniques that were used for the characterization of the present systems gave information on the assemblies of gemini peptides at different levels—from macroscopic to mesoscopic levels down to molecular levels—as well as on inter- and intramolecular interactions.

Gelling Behaviors, Mesoscopic Structures, and Supramolecular Structures. The matching between the gelling behaviors presented in Table 1 and the Krafft temperatures shown in Figure 3 confirmed that the gels of gemini $AcGly_pAsp$ were

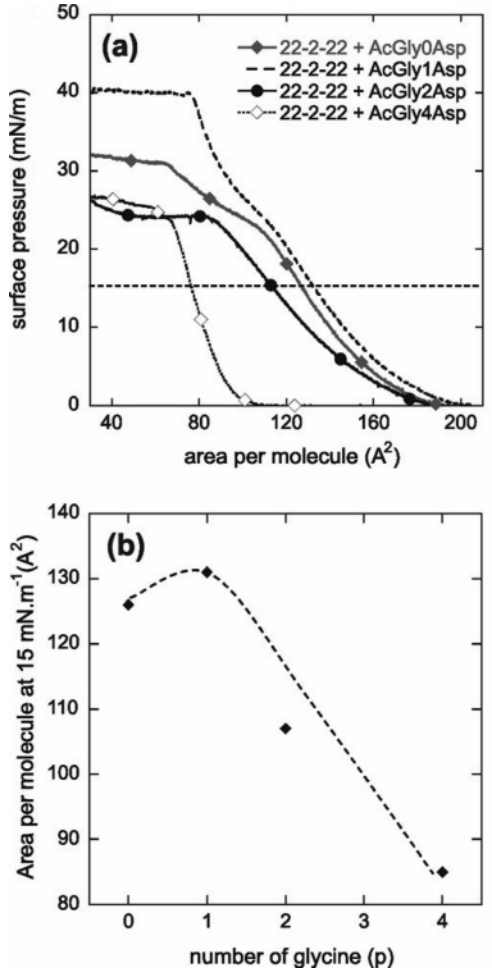

Figure 6. $\pi-A$ isotherm curves of 22-2-22 acetate on subphases with 6250 equivalent of AcGly$_p$Asp with $p = 0$, 1, 2, 4. The line is a guide for the eye.

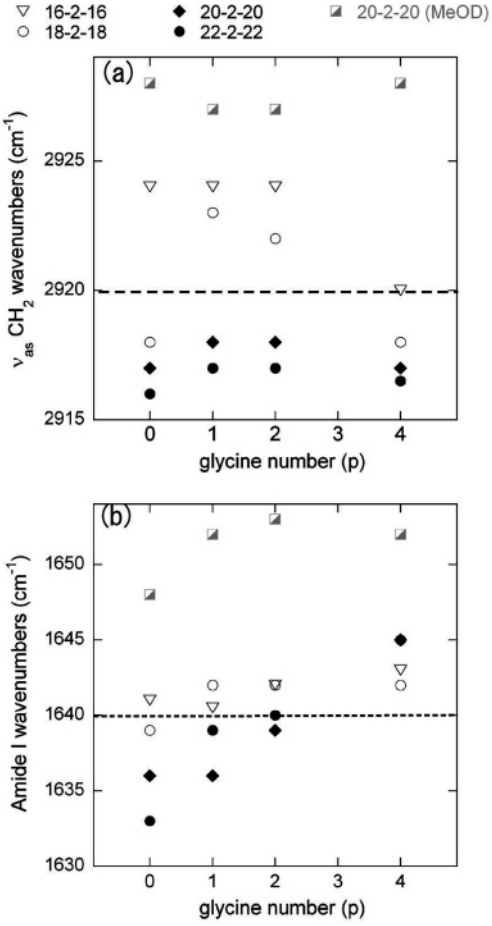

Figure 7. Peak positions for (a) CH_2 ν_{as} vibrations and (b) amide I vibration. Measurements were performed for C16, C18, C20, and C22 and for $p = 0-4$, all aged for 72 h. The results obtained with 20-2-20 AcGly$_p$Asp in deuterated methanol (which remains as solution) are shown for comparison.

observed only below the Krafft temperature, typical behavior for metastable physical gels.

The gels observed with gemini AcGly$_p$Asp showed three-dimensional networks of ill-defined structures on the order of submicrons. On the other hand, the interbilayer periodicity observed with SAXS measurements illustrated that this distance increased as the chain lengths were increased in both hydrated and dehydrated gels. The absolute values of these periodicities indicated that they were either interdigitated or tilted. The variation of the periodicity as a function of peptide length was much more complex. In the hydrated gels, they showed minima at glycine number 1 or 2. Such a behavior was not observed with dehydrated gels, where the periodicity showed a monotonic increase with peptide length. This suggests that the bilayers with low glycine numbers are much more hydrated than the gels with higher glycine numbers and they collapse to give much smaller periodicities when dried. This might indicate that, because of the intermembrane interaction, the water molecules were readily expulsed (see Figure 12) for the gels with high glycine numbers.

Molecular Organization. The presence of intermolecular interaction was then confirmed with infrared (IR) spectroscopy. Wavenumbers corresponding to both the stretching bands for CH_2 groups of hydrophobic chains and the amide I band decreased as gels were formed. The time difference in reaching the equilibrium value (much faster for CH_2 groups than for peptide groups) seemed to indicate that the aggregation was first driven by the assembling mechanism of gemini molecules, and then the organization of peptidic counterions followed afterward. These evolutions were not observed with the solutions (C16 and C18 with $p = 1$ and 2, and the methanol solution of 22-2-22 AcGly$_1$-Asp), which indicated that high ordering for *both* hydrophobic chains and peptidic counterions was needed for gel formation.

What was intriguing was the presence of the second peaks around 1670 cm^{-1} on top of the peak around 1645 cm^{-1}, observed mostly exclusively with gels with $p = 4$. These peaks were also absent when two peptidic counterions were complexed with a gemini molecule. An amide I peak around 1670 cm^{-1} had been shown as typical of a β-turn as confirmed by circular dichroism and NMR measurements.[18] Then, we may ask if it is related to the difference in the area per gemini molecule and per peptide chain. Since distances between gemini molecules are typically 7−9 Å^2, characteristic of two large headgroups (quaternary ammoniums), whereas distances between peptide chains forming hydrogen bonds is typically ∼4 Å, peptides complexed with gemini could not have strong hydrogen bonding networks which could explain the loose interaction characterized by a relatively high amide 1 band, ≥1636 cm^{-1} most of the time. However, for a long peptide AcGly$_4$Asp, they could better occupy the space by partially making a turn and disordered structures (see Figure 12). This would be inhibited when two peptides were complexed with one gemini molecule occupying much a larger area per molecule, which might explain the absence of the peak at 1670

(18) Gao, F.; Wang, Y.; Qiu, Y.; Li, Y.; Sha, Y.; Lai, L.; Wu, H. *J. Peptide Res.* **2002**, *60*, 75.

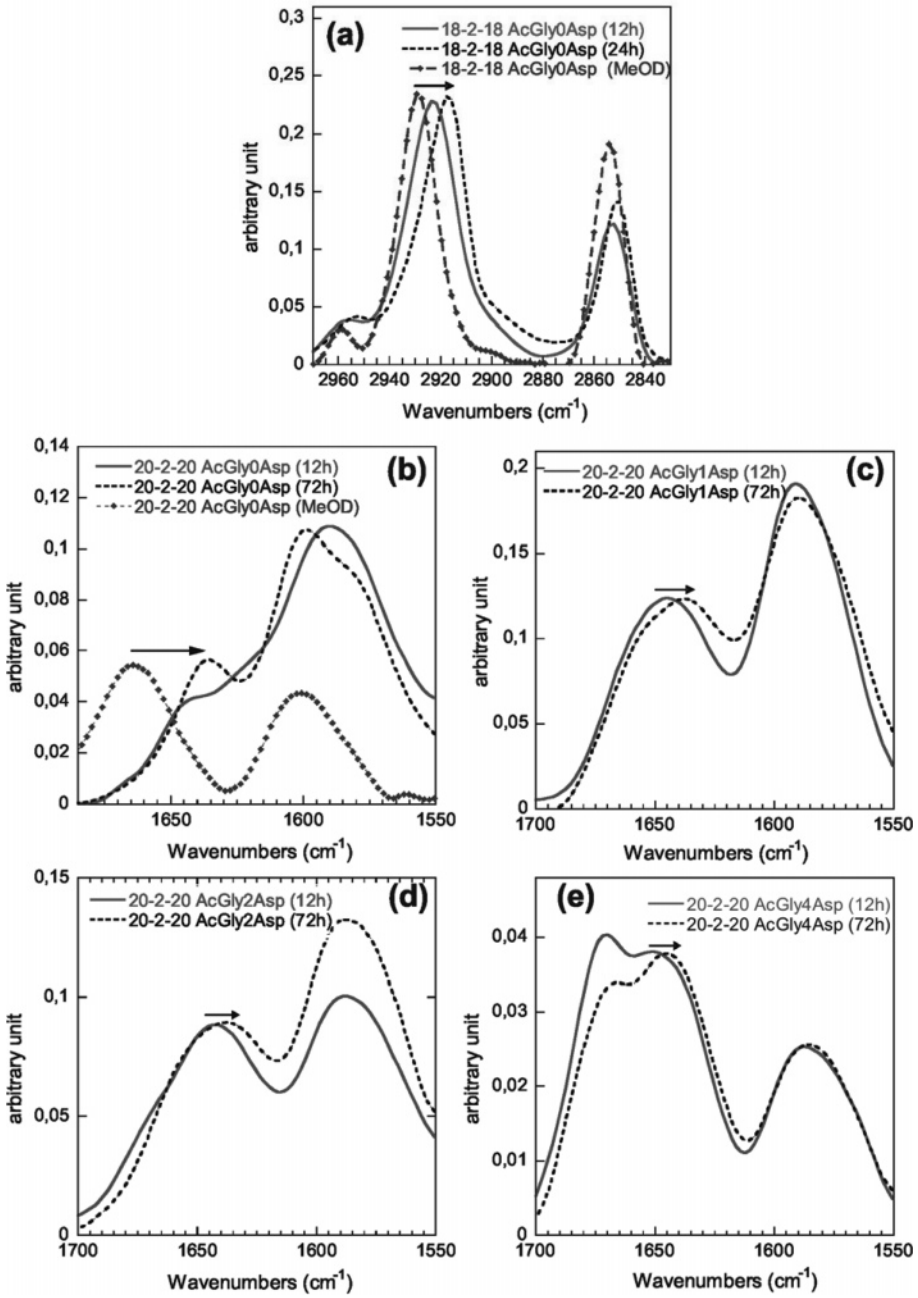

Figure 8. Typical wavenumbers corresponding to the stretching vibration of CH_2 decrease upon gel formation, which takes about 24 h, as shown for (a) 18-2-18 $AcGly_0Asp$. The amide I band also decreases with time, but much more slowly. For 20-2-20$AcGly_{0-4}Asp$, it took about 3 days (b−e) for them to reach the final values, whereas the corresponding CH_2 vibration bands were already at the low values (2917/2850 cm^{-1}) after a few hours.

cm^{-1} and a much higher periodicity observed by SAXS measurements.

Intermolecular Interaction, cmc, Krafft Temperature, SAXS, and Langmuir Film. The cmc measurements showed a clear effect of chain length: they decreased about an order of magnitude as the chain length was decreased by two carbons (per chain, therefore four carbons per gemini molecule), which was a typical behavior for ionic surfactants. On the other hand, the variation in glycine length did not seem to strongly influence the cmc. Values for a fixed chain length seemed to indicate that the cmc was mainly controlled by the hydrophobicity and ionic characteristics of the molecules.

The insensitivity to glycine length was not reflected by the Krafft temperature. The Krafft temperature increased about 15−20 degrees per two carbons, at a fixed glycine length. However, it did not show the monotonic variation with glycine length. For all the chain lengths investigated, it showed a minimum. This minimum was observed at $p = 2$ for C18 and at $p = 1$ for C22. The presence of such a minimum could be compared to the maximum of molecular area observed with surface pressure isotherms. For C18 and C20, molecular areas were maximum for $p = 2$ and 1, respectively. For the C22 gemini monolayer with subphase saturated with $AcGly_pAsp$, the behavior was much more enhanced, showing a maximum of the molecular area at $p = 1$.

Such behaviors may be described as follows. Both Krafft temperature and molecular area at the air−water interface were closely related to the intermolecular interaction at the interface of the aggregates. Such an interaction could be described as a cooperative effect between repulsion due to steric hindrance

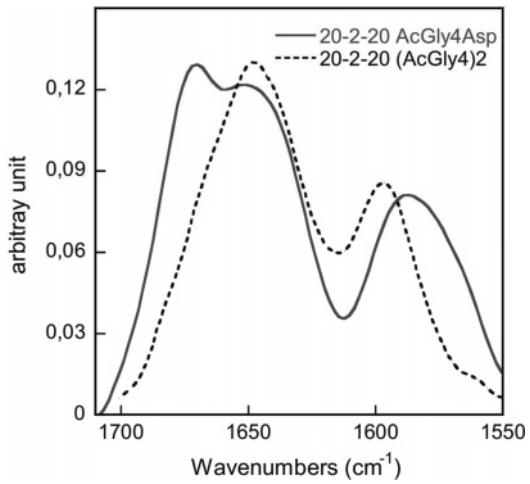

Figure 9. Amide peaks are compared for gemini complexed with one ($AcGly_4Asp$) or two $(AcGly_4)_2$ glycines. The peak at 1670 cm^{-1} is much more pronounced for gemini $AcGly_4Asp$ than for gemini $(AcGly_4)_2$.

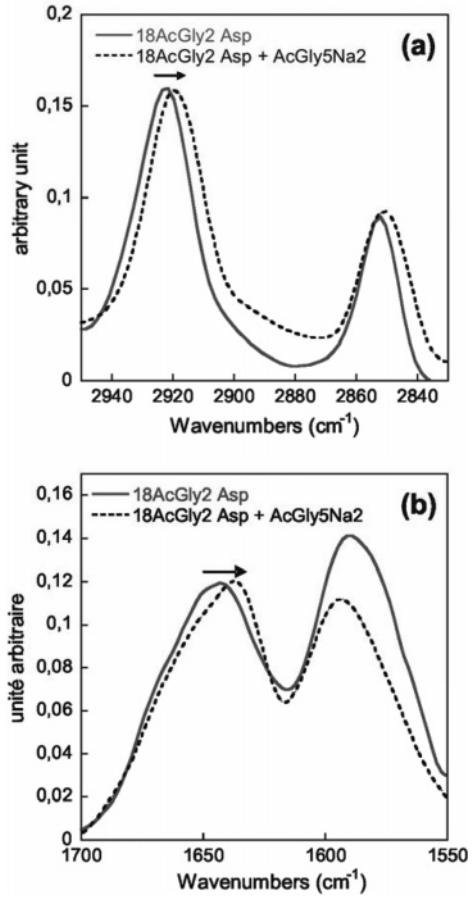

Figure 10. Effect of $AcGly_5Na$ added in the solution of 18-2-18 $AcGly_2Asp$ in (a) stretching vibration of CH_2 chains and (b) amide I bands. After 3 days, both domains show much better organization at 2922/2852 cm^{-1} (CH_2) and 1642 cm^{-1} (amide I) for 18-2-18 AcGly2Asp compared to 2920/2850 cm^{-1} (CH_2) and 1634 cm^{-1} (amide I) for 18-2-18 $AcGly_2Asp$ + $AcGly_5Na$.

(chains and peptides) and electric repulsion (ionic headgroups and counterions) and intermolecular attraction due to van der Waals interaction (chains) and hydrogen bonding (peptides). At a fixed chain length, as the peptidic length was increased, while the ionic repulsion remained the same, the steric hindrance and the intermolecular attraction both increased, which influenced

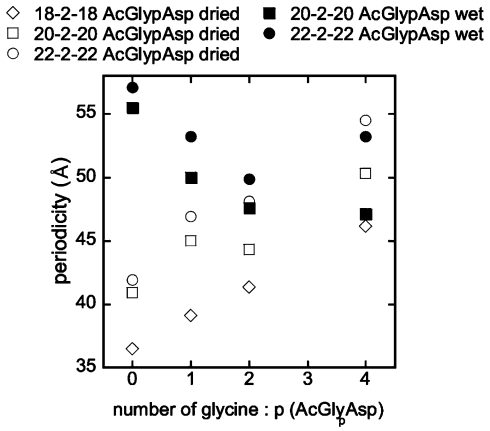

Figure 11. Interbilayer periodicity is shown for dehydrated and hydrated gels for different chain lengths (C18−C22) as a function of glycine number. For the dehydrated gels, the periodicity increases as the chain number and the peptide number increases, whereas the hydrate gels show minima at $p = 2$.

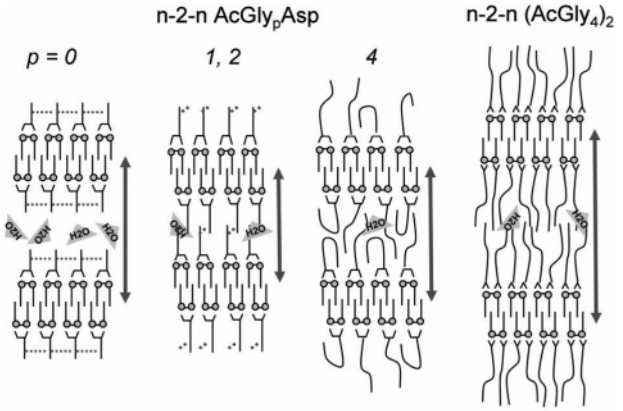

Figure 12. Schematic representation describing the variation of interbilayer distance as a function of peptide length for associated peptidic structures observed by infrared observations. For $p = 0$, each bilayer is individualized, and headgroups are well hydrated. For $p = 1, 2$, interbilayer interaction prohibits hydration, resulting in decreasing interbilayer distance. As the peptidic length is further increased, $p = 4$, the distance increases again, and peptides partially start to fold back, making turns. When two oligopeptides are complexed per gemini, much less area per peptide is available, prohibiting the formation of turns and increasing the interpeptidic distance.

the molecular area in the opposite sense. At short peptidic length ($p = 0, 1$), the steric and ionic repulsion won over, increasing the molecular area and the disorder of the molecular packing, and decreasing the Krafft temperature. As the peptides got longer, intermolecular attraction got stronger, thus decreasing the molecular area and increasing the Krafft temperature.

The peptide length with which the maximum molecular area and minimum molecular organization was observed is determined by the two antagonistic effects described above; therefore it varied with the chain length. This might be why the maximum molecular area was observed with $p = 1$ for C20 whereas for C18 a longer peptide length was needed.

Conclusion

Cationic gemini surfactants complexed with $AcGly_pAsp$ counterions are gelling agents of water when either the hydrophobic chains or the peptides are long enough. Microscopic observations show a network of membrane/fibrous structures. These structures are probably formed with periodic bilayer-type

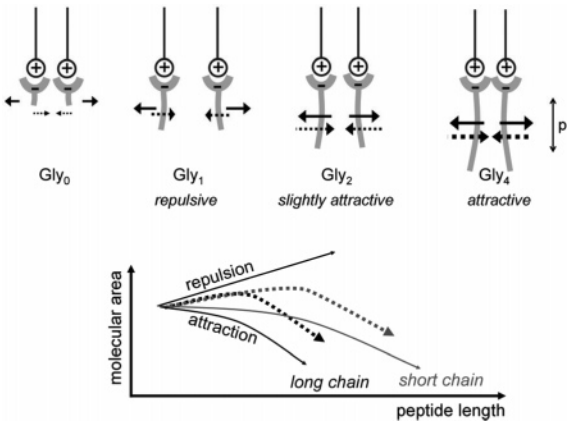

Figure 13. Illustration of the presence of antagonistic effects between repulsive and attractive interactions. As the peptide and hydrocarbon chain length increase, steric repulsion between molecules increases; in parallel, there is a strong attraction due to hydrogen bonding (interpeptides) and van der Waals interaction (interpeptides and inter gemini molecules).

structures, and their periodicity increases with hydrophobic chain length. They also show an increase with peptide length for dehydrated gels, but for the hydrated gels they show a minimum, indicating that, for short peptides, membranes are much more hydrated than they are for longer peptides which form an interbilayer interaction expulsing water molecules between bilayers.

Whereas the critical micellar concentration seems to be controlled mainly by the hydrophobicity of the molecules, the Krafft temperature and the molecular area at air−water interface show that the aggregation is probably a cooperative process between intercation/interanion repulsion and attractions due to sterical, ionic, hydrophobic, and hydrogen bonding interactions. FT-IR measurements suggest the formation of hydrogen bonding between the oligopeptidic counterions. For long peptides, $p = 4$, it seems that the discrepancy between areas occupied by gemini molecules and by AcGly$_p$Asp allows the oligoglycines to form a mixture of random structures and turns.

Acknowledgment. This work was supported by the CNRS, the University of Bordeaux I, and the Aquitaine region. The authors are grateful to B. Desbat and T. Buffeteau for useful suggestions on FT-IR spectroscopy.

LA053516A